# MEMs-Based OCT Endoscope

Timothy Perrier, McGill ID: 260959797

December 1, 2020

# 1 Abstract

The purpose of this project was to design a MEMs-Based OCT endoscope based on certain design constraints such as size and the field of view of the system. As this OCT device is small, it would be used to image smaller organs or tissues inside the body. Design of this system was done in the CodeV optical design software. This system has a 6.4 x 4.15 $mm^2$ field of view, a 5.15 mm working distance, and transverse resolutions being in the range of 20 $\mu$m to 25 $\mu$m at better resolution locations.

# 2 Introduction

Optical Coherence Tomography (OCT) is a non invasive biomedical imaging technique primarily used for *in-vivo* applications. It produces either 2-D or 3-D cross-sectional images of body tissue, depending on how many scanning axes the OCT device has. OCT systems are commercially available; however, they are mostly large tabletop systems used by ophtalmologists to examine patients' retinas. Endoscopic OCT systems focus on parameters such as the endoscope size, working distance, and transverse (lateral) resolution of the system [1] for imaging of internal organs and tissues.

Typically, OCT uses light from the infrared range because it has a penetration depth of several hundreds of microns into body tissue [2]. Figure 1 depicts a general diagram of an OCT system [3]. The input beam of light is split into a reference and sample arm using an optical beam splitter. In the sample arm, the beam is sent into a lens system and gets reflected onto a sample by a scanning mirror. The reference arm contains a mirror that moves along an axis to the equivalent depth of penetration in the sample arm. An interferometric component measures backscattered light from both the reference and sample arms. A depth profile is created from backscattered light This light interferes either constructively or destructively, and software uses this data to construct the cross-sectional image. Different tissue types reflect back different intensities of light, making it easy to differentiate between cell layers in tissue. An example OCT image can be observed in Figure 2 [2], and the difference between layers of tissue are easily distinguishable.

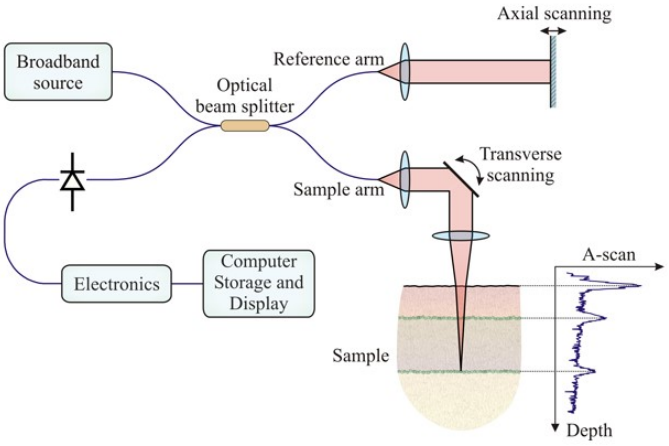


Figure 1: Diagram of a general OCT system.

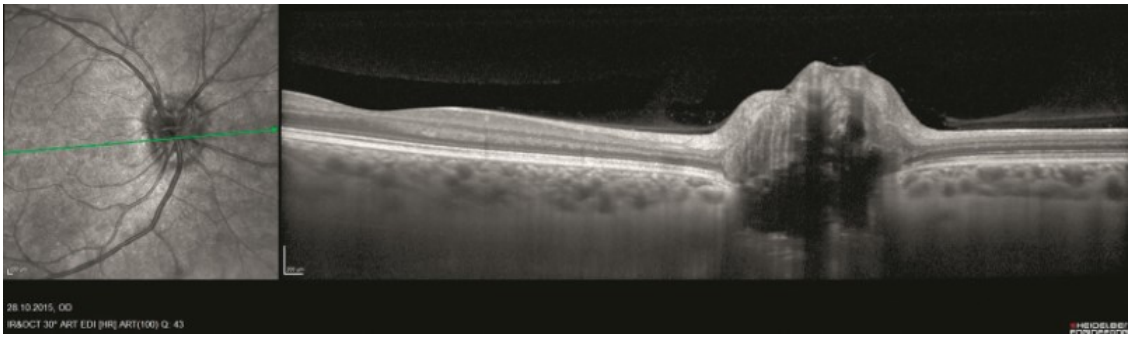

Figure 2: An exmaple OCT image (right) of a retina. The OCT image is scanned along the green line in the corresponding image on the left. The bulge in the OCT image is the optic nerve and it corresponds to the dark circle in the image on the left.

# 3 System Design

## 3.1 Constraints and Objectives

In this design, the input light wavelength is 830 nm. The objective is to achieve a 5 x 5 $mm^2$ field of view with the system being enclosed in a 7.5 mm diameter cylinder. For this design, only the beam delivery system into the sample arm was designed.

## 3.2 Components

The main challenges that OCT revolve around are small image sizes and the inability to image larger organs. These problems stem from a combination of short working distances and small scan angles. This design attempts to work around these challenges by using a C-Lens, which has a long working distance. The main compoents to this OCT design are a C-Lens and a dual-axis scanning mirror. Conventional OCT systems have been using GRIN lenses; however, a recent paper found that using a C-Lens is more cost efficient and has a much greater working distance [1]. Therefore, the design of this OCT system is adapted from the single C-Lens design used in this paper. This paper also provides a general diagram of a C-Lens and its parameters which can be seen in Figure 3 [1].

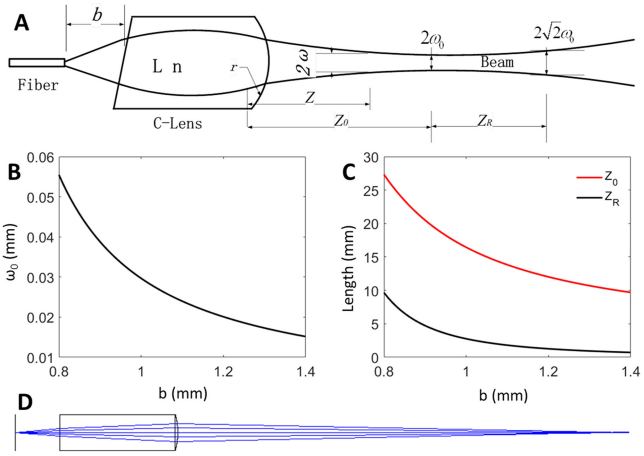


Figure 3: (a) General diagram of a C-Lens and its parameters; (b) Relationship between $\omega_0$ and $b$; (c) Relationship between $Z_0$, $Z_R$, and $b$; (d) Zemax simulation of the lens designed in [1] to show functionality of the C-Lens.

A C-Lens was chosen over a GRIN Lens combination due to a smaller form factor and longer focal length. C-Lenses are cylindrical rods with a flat surface on one end and a spherical surface on the other. The function of C-Lenses are for collimation and focusing of lasers. They have long focal lengths and working distances, and they have a lower cost than GRIN lenses. Parameters for this C-Lens were chosen, and the $\omega_0$ and $\frac{Z_0}{Z_R}$ values can be calculated using the following matrix computations [1].

$$T = \begin{bmatrix} 1 & 0 \\ \frac{n_0-n}{n_0 r} & \frac{n}{n_0} \end{bmatrix} \begin{bmatrix} 1 & L \\ 0 & 1 \end{bmatrix} \begin{bmatrix} 1 & 0 \\ 0 & \frac{n_0}{n} \end{bmatrix} = \begin{bmatrix} 1 & L\frac{n}{n_0} \\ \frac{n_0-n}{n_0 r} & [\frac{n_0-n}{n_0 r} L + \frac{n}{n_0}]\frac{n_0}{n} \end{bmatrix} \quad (1)$$

$$M = \begin{bmatrix} A & B \\ C & D \end{bmatrix} = \begin{bmatrix} 1 & z \\ 0 & 1 \end{bmatrix} T \begin{bmatrix} 1 & b \\ 0 & 1 \end{bmatrix} \quad (2)$$

The parameters for these matrices are as followed:

- L = length of C-Lens
- r = radius of curvature
- n = refractive index
- b = ditance between laser start and C-Lens

The C-Lens in this design has a 5 mm length, 5 mm radius of curvature. The glass material used for the lens is N-SF11 SCHOTT, giving the lens a uniform refractive index of 1.76. The resulting focal length of this C-Lens is approximately 6.55 mm.

In this design the scanning mirror is angled at 45° and tilts an additional ±10° relative to the sample surface. The mirror also tilts ±10° in the opposite axis. Figure 4 below depicts the mirror scan angles.

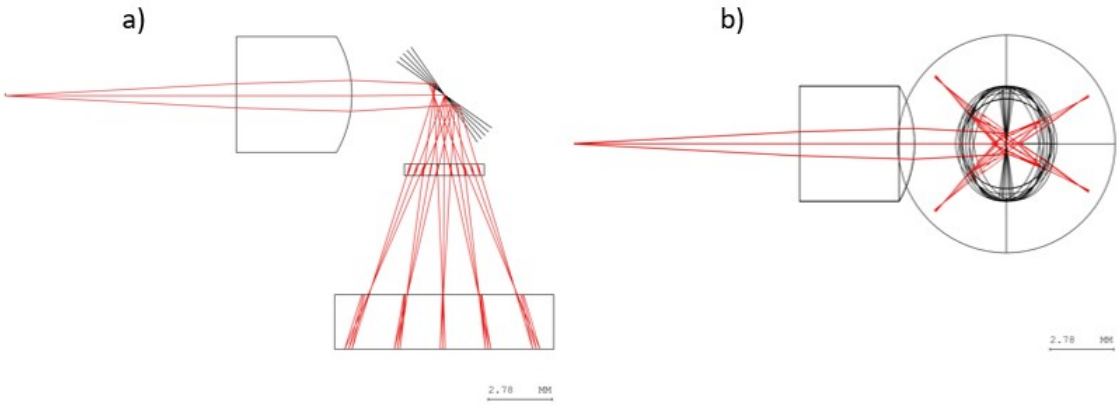


Figure 4: (a) A side view of the OCT system showing the mirror scanning 45° ±10° relative to the sample (b) A front view of the OCT system showing the mirror scanning ±10° relative to the face of the lens.

Underneath the mirror in Figure 4 are the viewing window and the sample surface. The viewing window has a radius of 3.5 mm, a thickness of 0.5 mm, and the material is NBK7 SCHOTT (n = 1.51). The sample has a refractive index of 1.33 because tissue refractive index is similar to that of water.

# 4 Results and Analysis

From analysing the CodeV model structures, the working distance is measured at approximately 7 mm. Depending on the application, this distance can be too short - especially for producing OCT images of retinal tissue. Although much larger than an endoscope such as this design, clinical tabletop OCT systems have working distances of around 25 mm [4].

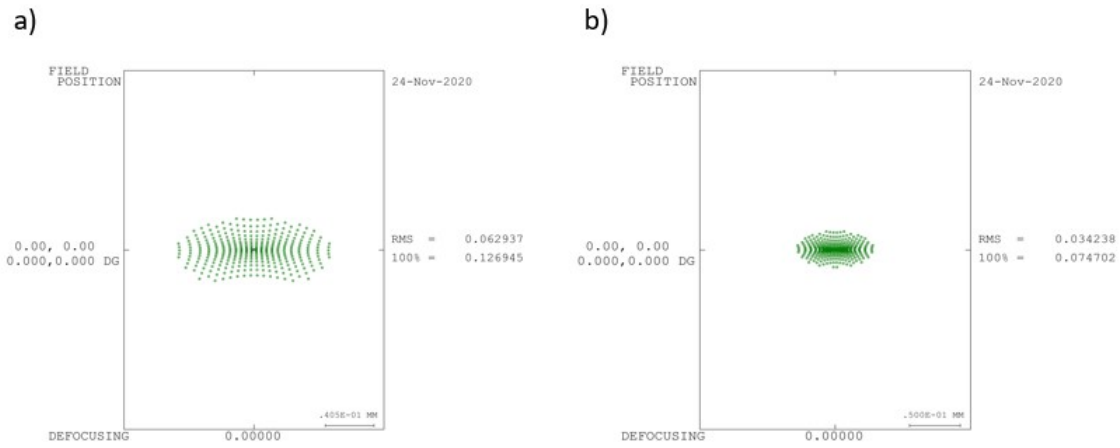


Figure 5: (a) Spot diagram at an Alpha tilt of 35° and no Beta tilt (b) Spot diagram at an Alpha tilt of 45° and no Beta tilt

Figure 5 depicts the spot sizes at various scan postions with a single scanning axis called Alpha. Using these spot diagrams and Equation (3) below, the transverse (lateral) resolution can be determined at different scan positions. The transverse rsolution is defined as the ability for an imaging system to distinguish between two points laterally (perpendicular to the beam) [5]. In OCT applications, this value is approximately the size of the beam waist along scan positions. In Figure 5 (a), the RMS value is 0.062937 and the scale bar is 40.5 $\mu$m. The RMS and scale bar values in Figure 5 (b) are 0.0342 and 50 $\mu$m respectively. The RMS value conveys information about the spread of points and the scale bar shows the overall spot size. Low RMS values are critical to having good resolution, and these obtained RMS values are small. Figure 5 (b) has the best transverse resolution of all the scan positions being between 50 $\mu$m and 60 $\mu$m. Although these are small transverse resolutions, an ideal transverse resolution for an OCT system is around 20$\mu$m to 25 $\mu$m [6], so improvements can still be made. The transverse resolution of an OCT system can be determined using the following equation, where $d$ is the spot size of the beam on the front surface of the objective lens [6].

$$\Delta x = \frac{4\lambda}{\pi}(\frac{f}{d}) = 1.27\frac{\lambda}{NA} \tag{3}$$

The value of $d$ can very depending on the divergence angle of the beam and the distance $b$ between the beam source and the lens, so Figure 6 shows how transverse resolution of this system changes based on the $d$ value. Values of 830 nm for $\lambda$ and 6.55 mm for $f$ are plugged in to the remaining parameters in Equation (3). Typically, commerical OCT systems have transverse resolutions between 20 $\mu$m to 25 $\mu$m, so the transverse resolution for this system can definitely be improved.

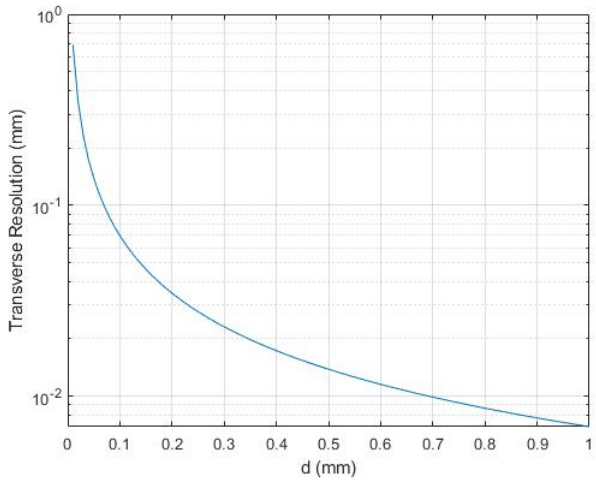


Figure 6: Relationship between transverse resolution of this OCT system and the beam spot size projected on the C-Lens, $d$.

Figure 7 depicts the spot diagrams when a second scanning axis is taken into account. The angle for the tilt of this axis is called Beta. Figure 8 shows the relative position of these spot diagrams in a 3-Dimensional view of the system. These scan positions were chosen to compare between the furthest corners of the scan. Right from the start, it can be seen that the resolution at these locations are much worse than the two spots analysed previously. This can be observed from both the RMS values and scale bars from both spot diagrams. The RMS values are 0.126 and 0.121 in Figure 7 (a) and (b), respectively. These values are much higher than the previously observed ones, and they indicate that spots are much less concentrated. The scale bars are also notably larger at 74.1 $\mu$m and 68.3 $\mu$m, indicating a lower resolution quality at extreme tilts of the mirror. This could potentially be fixed by implementing a curved mirror.

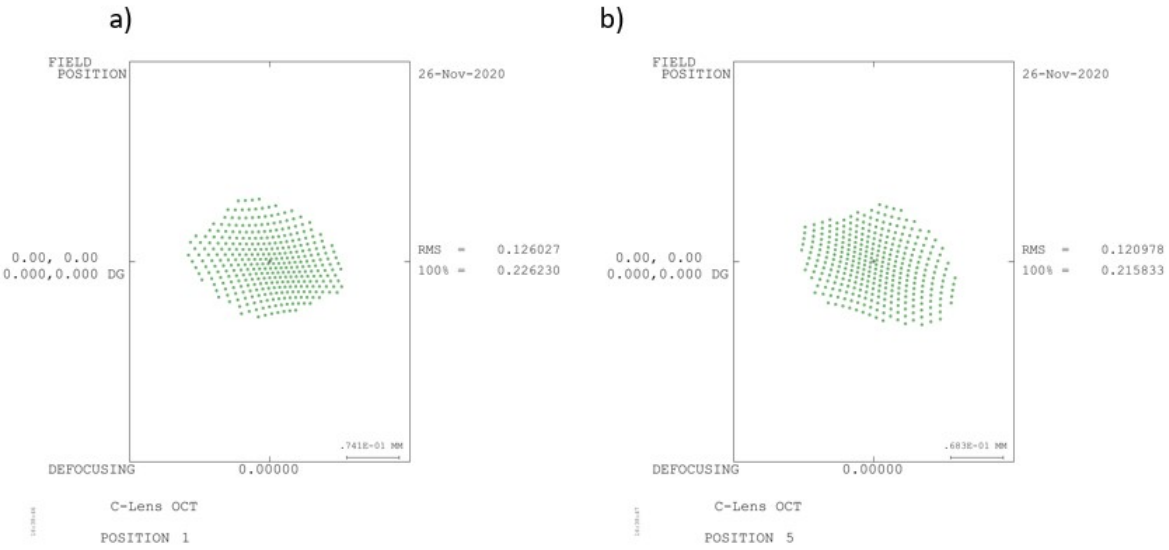


Figure 7: (a) Spot diagram for the position in Figure 8 (a) where the Alpha tilt is 35° and the Beta tilt is -10°; (b) Spot diagram for the position in Figure 8 (b) where the Alpha tilt is 55° and the Beta tilt is 10°

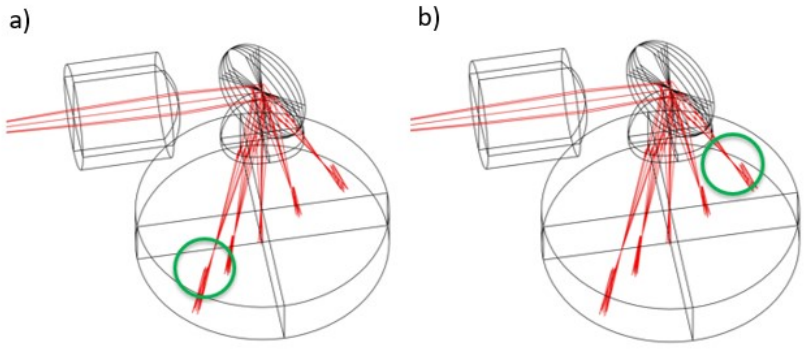


Figure 8: (a) Scan position with an Alpha angle of 35° and Beta -10°; (b) Scan position with an Alpha angle of 55° and Beta 10°

Using the Gaussian Beam Analysis tool produced the side vew of the OCT system in Figure 9. Parameters of 0.01 mm were used for both beam half-widths and a 0.4 mm wavefront radius of curvature was used for both the

X and Y directions. These parameters resulted in very small beam radii along the scan line. The center scan beam radii at the sample surface are 0.0088 mm and 0.0104 mm in the X and Y directions, respectively. Moving away from the center scan location, beam radii along the surface increases to around 30 $\mu$m to 40 $\mu$m. Figure 10 shows the beam intensity spread on the sample surface. The intensity has a good spread as seen by the scale bars of 0.192 mm. Having a small spread is crucial to reducing interference between points along a scan line. Other positions along the center scan line (Beta angle of 0°) have similar intensity spreads.

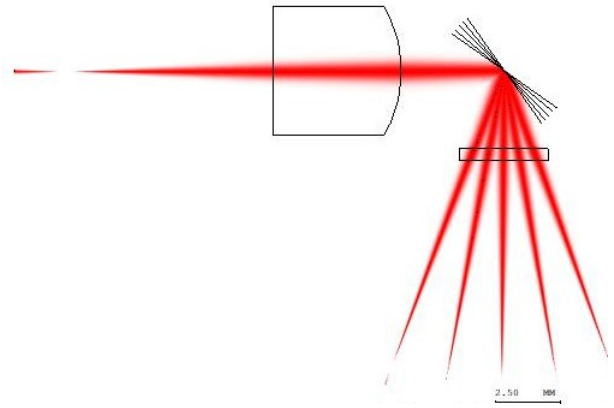


Figure 9: Trace of the Gaussian beam using the Gaussian Beam Analysis tool. The sample surface was ignored in this figure for simplicity.

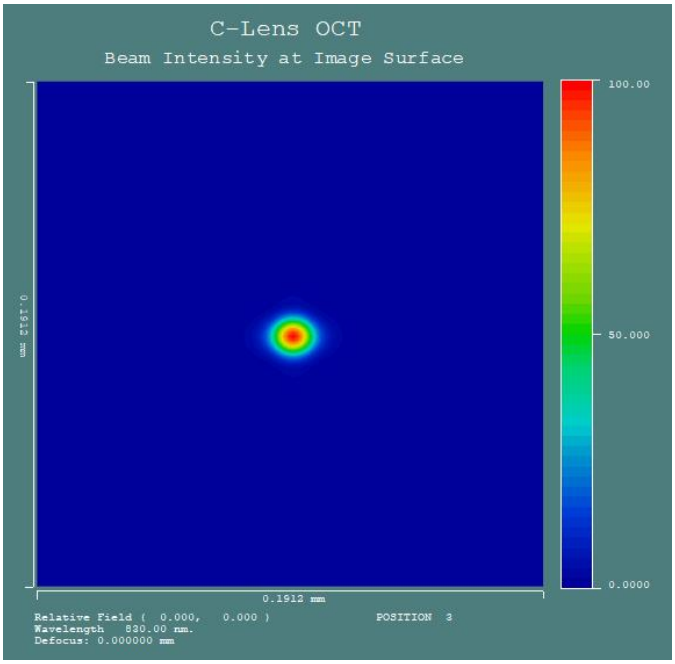


Figure 10: The spread of intensity of the beam spot at the sample's surface. This intensity spread is for the center scan.

# 5 Conclusion

The design objectives set at the beginning of this project were all met apart from the 5 x 5 $mm^2$ field of view. This OCT system is housed inside of a glass tube with a 7 mm diameter and uses infrared light of an 830 nm wavelength. The C-Lens enables this system to have a longer focal length than designs that use GRIN Lenses. From the intensity spectrum and numerical data from the Gaussian Beam Analysis the transverse resolution of this OCT system is approximately the same as that of commercial ones in the range of 20 $\mu$m. Spot diagram analysis showed how the resolution can still be improved - especially at the maximum scan positions. Using a curved mirror would most likely fix the trapezoidal-shaped field of view along with the issue of decreasing resolution as the scan moves away from the center. Although the results for this design are promising, it may not be practical in a physical model. This mainly stems from the Gaussian beam source being 10 mm away from the C-Lens which is quite a large distance in comparison to the size of

the entire system. The beam parameters were changed to make this distance feasible in the design; however, in physical applications or models it would not be ideal.

## 5.1 Future Work

The first edit to perform on this system would be to reduce the distance between the beam source and the C-Lens to make physical applications feasible. This would involve changing some of the C-Lens parameters such that it better focuses the beam. Future work on this project would include analysis of backreflected light from different tissue types in the sample. This analysis along with an interferometric setup could be designed in a different CodeV file.

# References


[1] S. Luo, L. Zhou, D. Wang, C. Duan, H. Liu, Y. Zhu, G. Li, H. Zhao, J. Tang, Y. Wu, X. An, X. Li, Y. Liu, H. Xie, and L. Huo. A miniature endoscopic optical coherence tomography probe based on c-lens. *IEEE Photonics Journal*, 10(5):1–10, 2018.

[2] Silke Aumann, Sabine Donner, Jörg Fischer, and Frank Müller. *Optical Coherence Tomography (OCT): Principle and Technical Realization*, pages 59–85. Springer International Publishing, Cham, 2019.

[3] Barry Cense and Michael Hackmann. Introduction to oct.

[4] Ruobing Qian, Oscar M. Carrasco-Zevallos, Shwetha Mangalesh, Neeru Sarin, Lejla Vajzovic, Sina Farsiu, Joseph A. Izatt, and Cynthia A. Toth. Characterization of long working distance optical coherence tomography for imaging of pediatric retinal pathology. *Translational Vision Science & Technology*, 6(5):12–12, 10 2017.

[5] Atif Qasim. Axial, lateral and temporal resolution.

[6] Dan P. Popescu, Lin-P'ing Choo-Smith, Costel Flueraru, Youxin Mao, Shoude Chang, John Disano, Sherif Sherif, and Michael G. Sowa. Optical coherence tomography: fundamental principles, instrumental designs and biomedical applications. *Biophysical Reviews*, 3, 2011.